Supplemental material for "Using Activated Transport in Parallel Nanowires for Energy Harvesting and Hot Spot Cooling"

Riccardo Bosisio, Cosimo Gorini, Geneviève Fleury, and Jean-Louis Pichard
Service de Physique de l'État Condensé, CNRS URA 2464, CEA Saclay, F-91191 Gif-sur-Yvette, France

I. RESOLUTION OF THE RANDOM RESISTOR NETWORK PROBLEM

Hereafter, we summarize the numerical method used to solve the random-resistor network problem[1–3]. The three-terminal setup configuration is reminded in Fig. 1, with emphasis on the hopping transport mechanism taking place in the NWs. Starting from a set of states i localized at positions x_i inside the NWs, with energies E_i and localization lengths ξ_i, we first evaluate the transition rates $\Gamma_{i\alpha}$ from the localized state i to the reservoir $\alpha = L$ or R, and Γ_{ij} from states i to j within the same wire (*inter*-wire hopping being neglected). They are given by the Fermi Golden rule as

$$\Gamma_{i\alpha} = \gamma_{i\alpha} f_i [1 - f_\alpha(E_i)] \quad (1)$$

$$\Gamma_{ij} = \gamma_{ij} f_i (1 - f_j)[N_{ij} + \theta(E_i - E_j)] \quad (2)$$

where f_i is the occupation probability of state i, $f_\alpha(E) = [\exp((E-\mu_\alpha)/k_B T_\alpha) + 1]^{-1}$ is the Fermi distribution of reservoir α, $N_{ij} = [\exp(|E_j - E_i|/k_B T) - 1]^{-1}$ is the probability of having a phonon with energy $|E_j - E_i|$ assisting the hop, and θ is the Heaviside function. In Eq. (1), $\gamma_{i\alpha} = \gamma_e \exp(-2x_{i\alpha}/\xi_i)$, $x_{i\alpha}$ denoting the distance of state i from reservoir α, and γ_e being a constant quantifying the coupling from the localized states in the NW to the extended states in the reservoirs. Usually, $\xi_i \approx \xi(\mu)$ is assumed and the rate γ_{ij} in Eq. (2) is simply given by $\gamma_{ij} = \gamma_{ep} \exp(-2x_{ij}/\xi(\mu))$, with $x_{ij} = |x_i - x_j|$ and γ_{ep} measuring the electron-phonon coupling. Since this approximation does not hold in the vicinity of the impurity band edges, where the localization lengths vary strongly with the energy, we use a generalized expression for γ_{ij} that accounts for the different localization lengths $\xi_i \neq \xi_j$ (see Ref.[4]).

By using Eqs. (1)-(2) and imposing charge conservation at each network node i, we deduce the N f_i's of the M independent NWs. The charge and heat currents flowing from reservoir α to the system can then be calculated as $I^e_\alpha = e \sum_i I_{\alpha i}$ and $I^Q_\alpha = \sum_i I_{\alpha i}(E_i - \mu_\alpha)$, where $I_{\alpha i} = \Gamma_{\alpha i} - \Gamma_{i\alpha}$ and e is the electron charge. In principle, the heat current $I^Q_P = (1/2)\sum_i I^Q_i$ coming from the phonon bath can be calculated as well but in the letter, we only investigated the behavior of the local heat currents $I^Q_i = \sum_j (E_j - E_i) I^N_{ij}$ with $I^N_{ij} = \Gamma_{ij} - \Gamma_{ji}$. Without loss of generality, we choose the right terminal R as the reference, i.e. we set $\mu_R = \mu$, $T_R = T$ and we impose on the left side $\mu_L = \mu + \delta\mu$, $T_L = T + \delta T$. Using the Onsager formalism, we relate the particle (I^e_L) and heat (I^Q_L) currents computed in linear response to the small imposed bias $\delta\mu$ and δT[5]. This allow us to deduce the thermoelectric coefficients G, K^e and S.

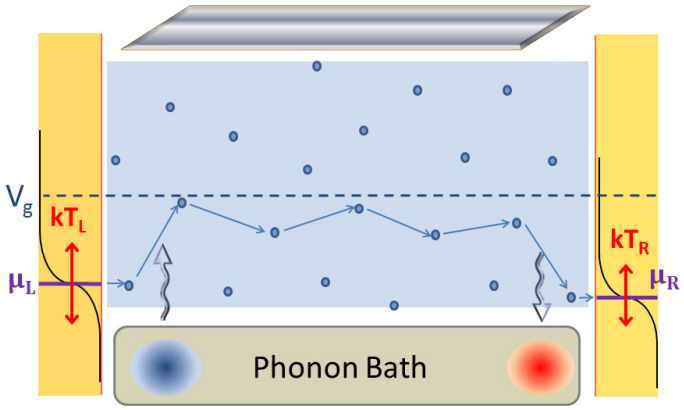

FIG. 1. Phonon-assisted hopping transport through the localized states (dots) of a disordered NW connected to two electrodes L and R, and to a phonon bath. The electronic reservoirs L and R are thermalized at temperatures $T_{L[R]}$ and held at electrochemical potentials $\mu_{L[R]}$ (their Fermi functions are sketched by the black curves at both sides). A metallic gate (shaded grey plate drawn on top) allows to shift the NW impurity band (blue central region). Here, the gate potential V_g is adjusted such that electrons tunnel in and out of the electronic reservoirs near the lower edge of the impurity band. Therefore, electrons tend to absorb phonons at the entrance in order to reach available states of higher energies, and to emit phonons on the way out. The two wavy arrows indicate the local heat flows between the NW electrons and the phonon bath. They give rise to a pair of cold (blue) and hot (red) spots in the substrate beneath the NW (in the deposited setup configuration).

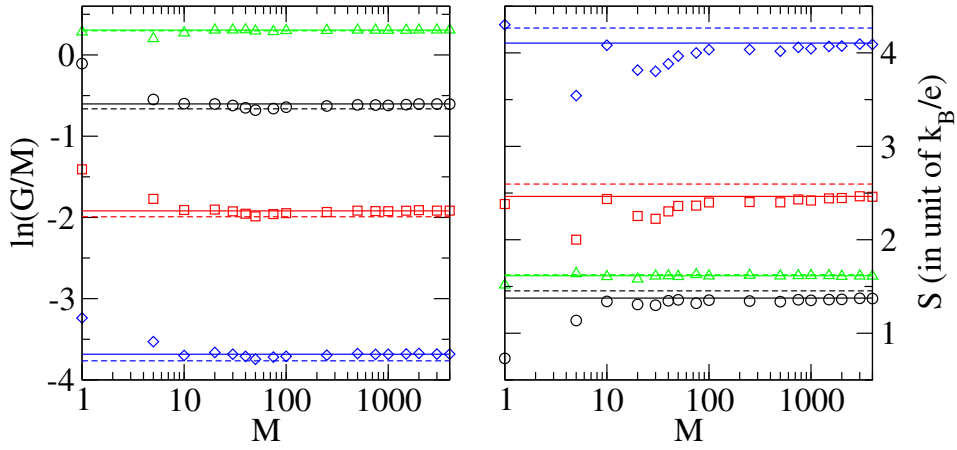

FIG. 2. (Color online) Convergence of G/M (left, in units of $e^2/\hbar$) and S (right) with the number M of parallel NWs. Symbols correspond to $V_g = 1.9\,t$ (○), $2.1\,t$ (□) and $2.3\,t$ (◇) at $k_BT = 0.1\,t$, and $V_g = 1.9\,t$ at $k_BT = 0.5\,t$ (△). The horizontal lines indicate the corresponding mean values (dashed lines) and typical values (full lines) of $\ln G$ and S of a single wire ($M = 1$). Parameters: $W = t$, $\gamma_e = \gamma_{ep} = t/\hbar$ and $L = 450a$.

II. SCALING OF THE THERMOELECTRIC COEFFICIENTS WITH THE NUMBER OF NANOWIRES

The typical conductance G_0 and thermopower S_0 of a single NW were studied in Ref.[4]. They are defined as the *median* of the distribution of $\ln G$ and S, obtained when considering a large statistical ensemble of disorder configurations. In Fig. 2 we show that, if the system is made of a sufficiently large number $M > M^*$ of parallel NWs, the *overall* electrical conductance scales as the number of wires times the typical value ($G \approx M\,G_0$), while the thermopower averages out to the typical value of a single wire ($S \approx S_0$). For completeness the *mean* values are also shown and seen to be a less accurate estimate. As expected, convergence is faster at higher temperatures. Note that identical results have been obtained for the electronic thermal conductance $K^e \approx MK_0^e$ (not shown).

III. SIZE EFFECTS

We have investigated the effects on the various transport coefficients G, K^e and S, the power factor $\mathcal{Q}$, and the electrical figure of merit Z_eT, of varying the length L of the NWs. The results are shown in Fig. 3, for three values of the temperatures $k_BT = 0.1t, 0.5t$ and $1.0t$, and for two configurations corresponding to bulk ($V_g = t$) and edge transport ($V_g = 2.5t$). We observe that they are essentially always size-independent, for μ inside the impurity band and also around its edge. The only exception is the electrical conductance at low temperatures and in the case of edge transport: this causes the electrical figure of merit Z_eT to decrease in this regime (◦ in Fig. 3(d)) roughly as $1/L$. However, being interested in the regime of temperatures where the power factor is largest ($k_BT \simeq 0.5t$), we can conclude that the size effects on the results shown in the letter are completely negligible. Also, we note that the small fluctuations observed especially at the smallest sizes are a consequence of having taken a finite number of parallel NWs (M=150): they would vanish in the limit M$\to\infty$ due to self-averaging.

IV. ON THE DEPENDENCE ON THE COUPLINGS γ_e AND γ_{ep}

In this section, we investigate how the transport coefficients G, K^e and S, the power factor $\mathcal{Q} = S^2G$ and the electrical figure of merit $Z_eT = S^2GT/K^e$ depend upon varying the couplings γ_e and γ_{ep} of the localized states with the electrodes and the phonon bath, respectively. We introduce the notation $\alpha \equiv \gamma_{ep}/\gamma_e$. We first notice that if α is kept fixed, the electrical conductance G and the electronic thermal conductance K^e are strictly proportional to γ_e, while the thermopower S is independent of it. This behavior is a direct consequence of the formulation of the random resistor network problem and can be seen at the stage of writing the equations (see Ref.[4]), before solving them numerically. Therefore, for any fixed α, $\mathcal{Q}/\gamma_e$ and Z_eT are necessarily independent of the choice of γ_e. We thus find that G/γ_e, K^e/γ_e, S, $\mathcal{Q}/\gamma_e$ and Z_eT are functions of the single parameter α, and not of the couple of parameters γ_e and γ_{ep} separately. Those functions are plotted in Fig. 4(a)-(c) for two different temperatures. The conductances, the power factor and the figure of merit increase with α (as long as lack of phonons is a limiting factor to transport

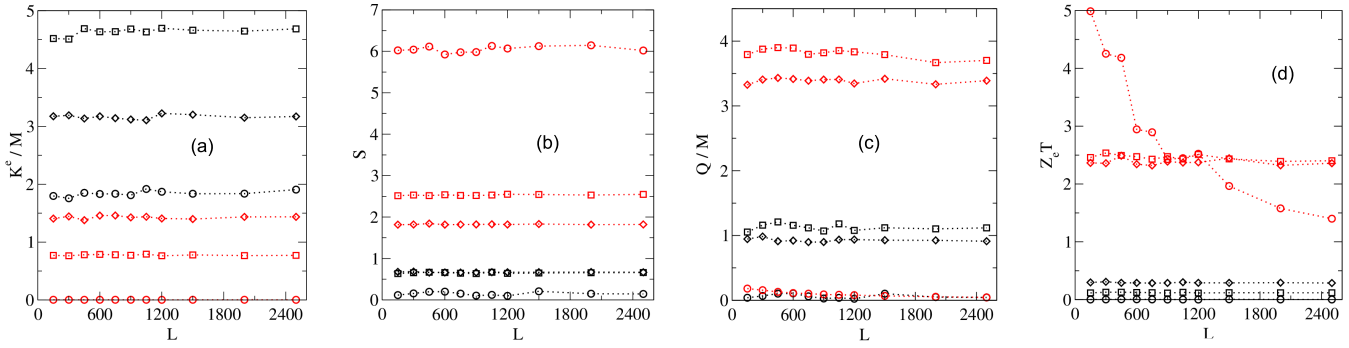

FIG. 3. (Color online) Behavior of the transport coefficients as function of the NWs size L (in units of the spacing a). Panels from left to right show (a) the rescaled electronic contribution to the thermal conductance K^e (in units of $k_B t/\hbar$), (b) the thermopower S (in units of k_B/e)), (c) the rescaled power factor $\mathcal{Q}$ (in units of $k_B^2/\hbar$) and (d) the electrical figure of merit Z_eT. In all the four panels, different symbols correspond to $k_BT = 0.1t$ (circles), $k_BT = 0.5t$ (squares) and $k_BT = t$ (rhombus), while different colors refer to the case of bulk transport ($V_g = t$, black) and edge transport ($V_g = 2.5t$, red). Dotted lines are guides to the eye. Other parameters are fixed to $W = t$ and $\gamma_e = \gamma_{ep} = t/\hbar$.

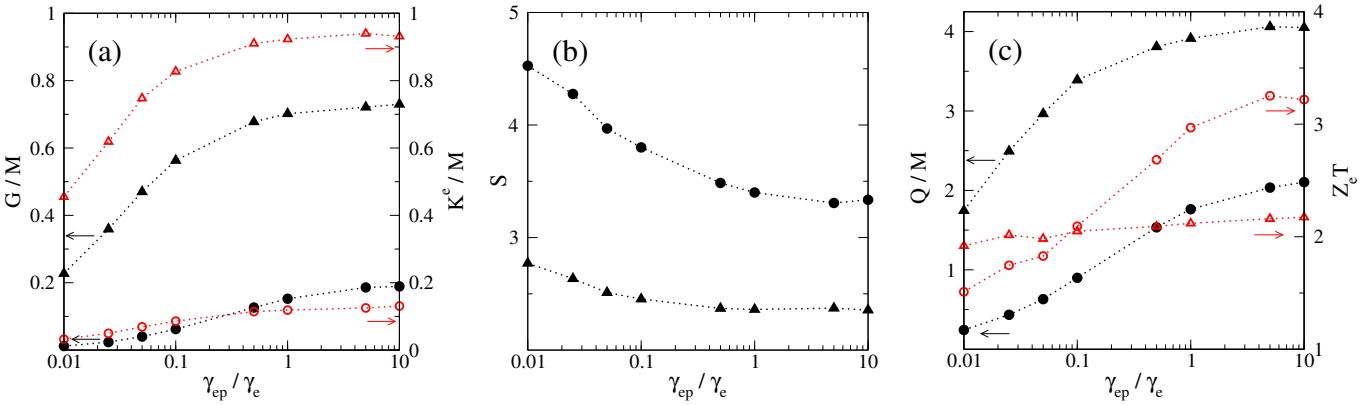

FIG. 4. (Color online) Dependency of G, K^e, S, $\mathcal{Q}$ and Z_eT on the ratio γ_{ep}/γ_e. (a) Electrical (G/M, black full symbols) and thermal (K^e/M, red empty symbols) conductances, in units of $e^2/\hbar$ and $k_Bt/\hbar$ respectively. (b) Thermopower in units of k_B/e. (c) $\mathcal{Q}/M$ in units of $k_B^2/\hbar$ (black full symbols) and Z_eT (red empty symbols). In all panels, different symbols correspond to $k_BT = 0.2t$ (circles) and $k_BT = 0.5t$ (triangles), while dotted lines are guides to the eye. Data have been plotted for a given set of $M = 150$ parallel NWs of length $L = 450a$, with $\gamma_e = t/\hbar$, $W = t$ and $V_g = 2.4t$. Note that when $\gamma_{ep} \gtrsim \gamma_e$ all these coefficients are nearly constant.

through the NWs), while the thermopower decreases. All of them tend to saturate for $\alpha \gtrsim 1$. This shows us, *inter alia*, that $\mathcal{Q}/\gamma_e$ and Z_eT are essentially independent of γ_e and γ_{ep} if $\gamma_{ep} \gtrsim \gamma_e$ and that they only deviate slowly from this limit if $\gamma_{ep} < \gamma_e$. Such a robustness of $\mathcal{Q}/\gamma_e$ and Z_eT to variations of γ_e and γ_{ep} reinforces the impact of the results shown in the letter.

V. HOT SPOTS

In this section, we provide more details concerning the effect of generating hot and cold spots using a semiconductor NWs-based device in the field effect transistor configuration. As stated in the letter, each NW exchanges *locally* a certain amount of heat with the substrate. The global effect of substrate heating/cooling is visible after summing the heat currents inside areas of size $\approx \Lambda_{ph}$, the (inelastic) phonon mean free path, which is a measure of the thermalization length in the substrate.

Before detailing this, we illustrate in Fig. 5 an example of the map of the *raw* heat currents I_i^Q locally exchanged with the substrate. The horizontal coordinate is the position along the NW (in units of a, the average distance between localized states), while the vertical one labels each NW. In this case, we see that the I_i^Q's fluctuate between positive and negative values at random positions of the substrate, and thus no net effect emerges.

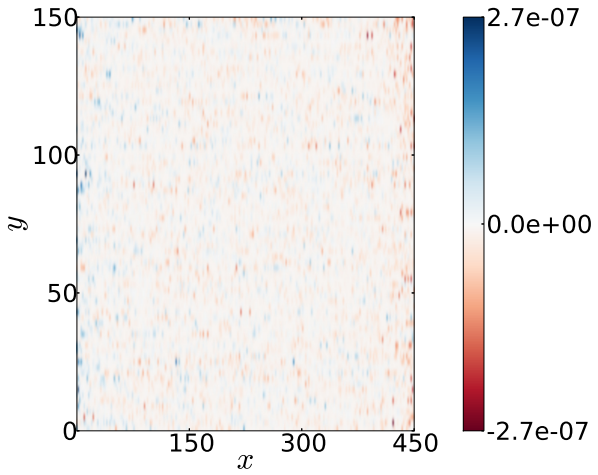

FIG. 5. Map of the local heat currents I_i^Q exchanged between the NWs and the substrate at each NWs site $i = (x, y)$, for $k_BT = 0.05t$ and $V_g = 2.25t$. The presence of hot and cold spots is hidden by the fluctuations. They emerge when the raw I_i^Q data are summed up within areas of size $\Lambda_{ph} \times \Lambda_{ph}$. Parameters: $M = 150$, $L = 450a$, $W = t$, $\gamma_e = \gamma_{ep} = t/\hbar$ and $\delta\mu = 10^{-5}t$.

The formation of the hot and cold spots is a process which becomes visible only upon summing in a single term $\mathcal{I}^Q_{x,y}$ all the contributions I_i^Q coming from states i located in a small area around the point of coordinates (x, y). Physically, the typical size of those areas corresponds to the thermalization length of the substrate. It is given by the inelastic phonon mean free path Λ_{ph}. This mean free path may be different for different phonon wavelengths, and while it does not change much around room temperatures, it can vary significantly at lower (still not vanishing) temperatures. It is possible to relate Λ_{ph} to the *dominant* phonon wave length[6] as $\Lambda_{ph} = 300\lambda_{ph}^{dom}$, where the coefficient 300 is for SiO_2 and may be different for other materials. This allows the calculation of the mean free path, once λ_{ph}^{dom} is known. According to Refs.[7,8], the latter can be estimated as

$$\lambda_{ph}^{dom} \simeq \frac{hv_s}{4.25k_BT}, \tag{3}$$

where h is the Planck constant. Taking $v_s = 5300\,\mathrm{m/s}$ the sound velocity in SiO_2[8], we can easily deduce $\lambda_{ph}^{dom} \simeq 0.2\,\mathrm{nm}$ from which $\Lambda_{ph} \simeq 60\,\mathrm{nm}$ at room temperature $T = 300\,\mathrm{K}$. Values of Λ_{ph} at other temperatures follow immediately from the temperature dependence in Eq. (3). We shall stress that the real values of Λ_{ph} may differ from our prediction by a small numerical factor, which however is not important within our qualitative approach. To convert these lengths in the units used in the letter, we assume the average distance between localized states $a \approx 3.2\,\mathrm{nm}$ in highly doped silicon NWs, which together with $t/k_B \approx 150K$ allows us to estimate for example $\Lambda_{ph} \approx 75a$ at $T = 0.5t/k_B = 75\,\mathrm{K}$.

In Fig. 6, we consider a set of $M = 150$ parallel NWs of length $L = 1500a \approx 4.8\mu\mathrm{m}$ with interspacing $15a \approx 50\,\mathrm{nm}$ among them. This choice of interspacing value corresponds to an array made of NWs of 10 nm diameter with 20% packing density. We show in the figure how $\mathcal{I}^Q_{x,y}$ vary spatially with the positions x, y in the substrate below the two-dimensional array of parallel NWs. Data are given for two different values of the temperature (top/bottom) and of the gate voltage (left/right). The top panels are the same as those presented in Fig. 2 of the letter. In this case, $T = 0.25t/k_B = 37.5\,\mathrm{K}$ and $\Lambda_{ph} \approx 150a$. Data show us that the hot and cold spots are visible only in presence of a large gate voltage, when the distribution of the energy states in the NWs is strongly asymmetric with respect to μ. The bottom panels of Fig. 6 show how the heat maps are modified when the temperature is doubled to $T = 0.5t/k_B \approx 75\,\mathrm{K}$. According to the prescription briefly discussed above, $\Lambda_{ph} = 75a$ in this case. The fact that the surface inside which the heat currents are summed up is now smaller is compensated by a smoothing of the I_i^Q's fluctuations at larger temperature. This makes the hot and cold spots still clearly visible and well-defined in panel (d).

[1] A. Miller and E. Abrahams, Phys. Rev. **120**, 745 (1960).
[2] V. Ambegaokar, B. I. Halperin, and J. S. Langer, Phys. Rev. B **4**, 2612 (1971).

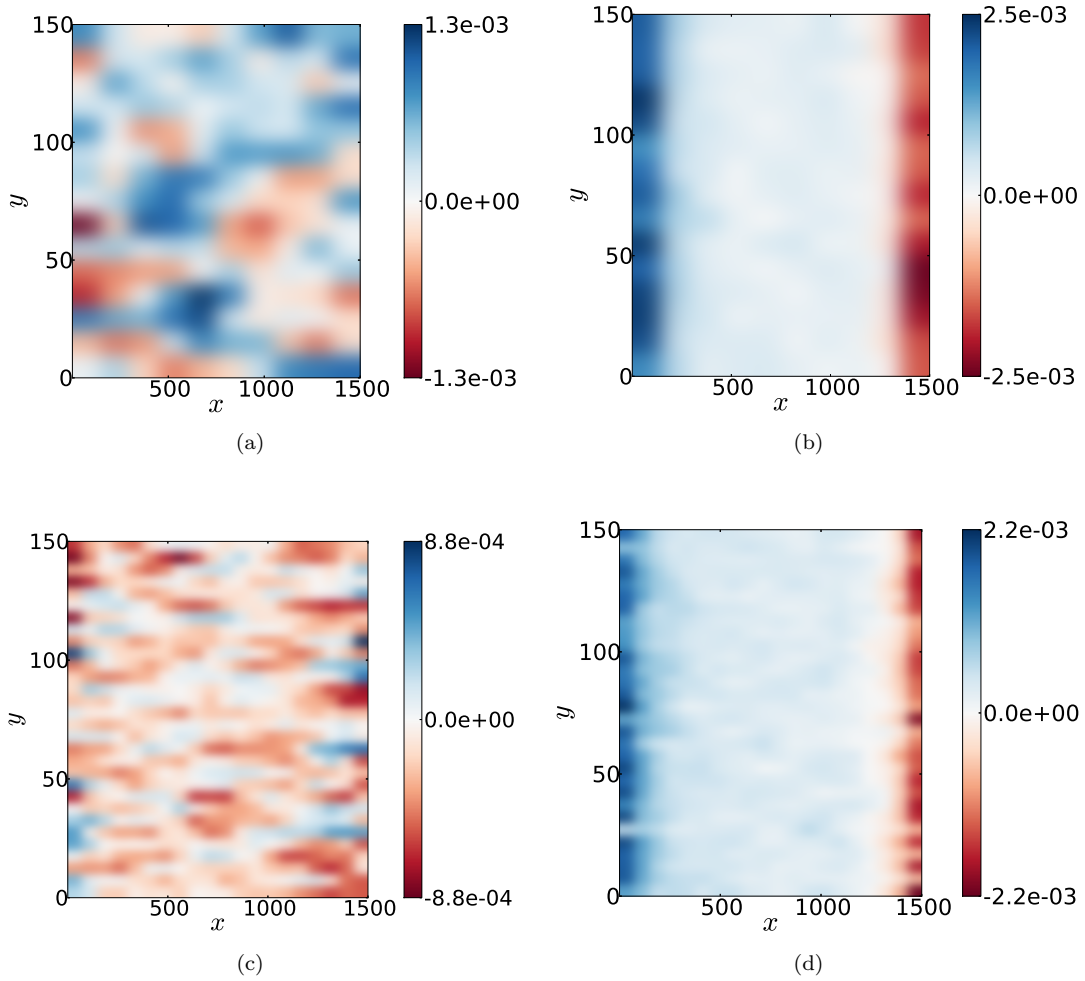

FIG. 6. Map of the local heat exchanges $\mathcal{I}^{Q}_{x,y}$ between the NWs and the phonon bath (substrate), in units of $t^2/\hbar$. Various panels correspond to different gate voltages and temperatures: $V_g = 0.0$ in (a) and (c), $V_g = 2.25t$ in (b) and (d), $k_BT = 0.25t$ in (a) and (b), $k_BT = 0.5t$ in (c) and (d). The heat currents have been summed inside areas of size $\Lambda_{ph} = 75a$ for $k_BT = 0.5t$ and $\Lambda_{ph} = 150a$ for $k_BT = 0.25t$, as explained in the text. Note that the formation of hot and cold spots at the boundaries of the NWs is clearly visible for both temperatures when V_g is tuned in order to probe their band edges ((b) and (d)), while no net effect is evident in absence of any gate voltage ((a) and (c)). In all panels, data have been plotted for $M = 150$ NWs of length $L = 1500a$ with interspacing $15a$. Other parameters are $W = t$, $\gamma_e = \gamma_{ep} = t/\hbar$ and $\delta\mu = 10^{-3}t$.

[3] J.-H. Jiang, O. Entin-Wohlman, and Y. Imry, Phys. Rev. B **87**, 205420 (2013).
[4] R. Bosisio, C. Gorini, G. Fleury, and J.-L. Pichard, arXiv:1403.7475(2014).
[5] H. Callen, *Thermodynamics and an Introduction to Thermostatics* (John Wiley and Sons, New York, 1985).
[6] R. O. Pohl, X. Liu, and E. Thompson, Rev. Mod. Phys. **74**, 991 (2002).
[7] T. Klitsner and R. O. Pohl, Phys. Rev. B **36**, 6551 (1987).
[8] J. M. Ziman, *Electrons and Phonons: The Theory of Transport Phenomena in Solids* (Clarendon Press, 1996).